

Modeling dam break granular flows

C. Di Cristo & A. Leopardi

DiMSAT, University of Cassino, via G. Di Biasio 43, 03043 Cassino (FR), Italy.

M. Greco

DIGA, University of Naples "Federico II", via Claudio 21, 80125 Napoli, Italy

ABSTRACT: In this paper a dry granular dam break phenomenon is investigated comparing experimental and numerical results. The experiments were performed reproducing the sudden collapse by the retaining wall of dry grains of sand in a rectangular horizontal channel with different initial dam height values. A depth-integrated two-phase flow model, developed for sediment transport in fluid flows in unsteady conditions, is used for simulating the experiments. In particular, the investigation is focused on how to reproduce the effect of resistive forces on a dam break granular flow. The proposed model accounts for sediment particles collisional shear stress through a kinetic scheme and frictional stress through a Coulomb-like behavior. The comparison between numerical model prediction and experimental evidence show a very good agreement of the front position development and an enough reproduction of the free surface profiles. These results demonstrate that the considered model, even if developed for sediment transport in fluid flows, is able to reproduce with a unified approach also the dry granular material behavior. Moreover, the results show that expressing the resistance as sum of both collisional and frictional stresses is a good option for modeling dry granular dam break phenomena with a depth integrated continuum approach.

Keywords: Dam break wave, Friction, Granular flows

1 INTRODUCTION

The dam break phenomenon, that arises following the sudden removal of a vertical barrier, is not only a classical issue in fluid mechanics, but represents also an important problem in engineering applications, dealing with catastrophic flows of water or sand mixtures. Dam break was widely investigated also considering different fluids or granular materials (e.g. Frenette et al. 2002, Kerswell 2005, Chanson et al. 2006, Capart & Young 1998, Fraccarollo & Capart 2002, Spinewine & Zech 2007).

The main goal of the present study is to apply a depth integrated model, developed for sediment transport in fluid flows, for simulating a dry dam break phenomenon, in order to verify its performances in reproducing with a unified approach also dry granular material behaviour.

Development of numerical models for sediment transport and bed evolution in unsteady river flows has experienced a growing attention (e.g. Graf 1998). An important feature while developing a new model is to show that it is correct and

reasonably robust in its application of basic physical principles. A usual test is to verify sediment transport models in clear water conditions, conversely in this article only the solid fraction is considered. In particular, the two-phase flow model, developed by Greco et al. (2008) for simulating sediment transport and bed evolution in unsteady condition, is used for reproducing laboratory dry granular dam break tests. Particular attention is focused on how to model the effect of resistances in granular flows.

About the understanding of the dynamic of granular material, significant progress has been made on the study of granular flows down a slope using depth averaged continuum equations with various different ways of reproducing the effect of friction (Savage & Hutter 1989, Pouliquen 1999). Regarding transient situations, some experiments have been conducted considering the instantaneous release of a stationary cylindrical column of dry granular material on a horizontal plane (Lube et al. 2004, Lajeunesse et al. 2004). Despite the complexity of the dynamics, simple scaling laws have been found for describing the final deposit

configurations. About two-dimensional dam break, experimental investigations are reported in Lube et al. (2005) and Balmforth & Kerswell (2005). Recently, Roche et al. (2008) compare dam break experiments realized with water, fluidized and dry granular flows. The authors show a water-like behaviour of initially fluidized granular flows, with meaningful differences respect to dry material.

In the present work the behaviour of a granular material in a transient situation on an horizontal surface is analyzed. In particular, cohesionless dry grains, without interstitial fluid effect are considered. The granular material is assumed to be in a liquid regime, in which the material flows like a liquid and the sediment particles interact both by collisions and friction. Laboratory experiments were performed reproducing the sudden collapse by the retaining wall of dry grains of sand in a rectangular channel, using different initial column heights. The results of numerical model simulation are compared with the experimental data.

2 THE MATHEMATICAL MODEL

The model proposed by Greco et al. (2008), developed for sediment transport, expresses conservation of mass and momentum for both water and solid phases. In the application to granular flows here presented, only the equations relative to the solid phase are used.

On the assumption of hydrostatic pressure distribution, considering a layer of material flowing over a rigid surface and assuming no cross-stream variation of the depth, conservation of mass and momentum are expressed by:

$$\frac{\partial h}{\partial t} + \frac{\partial hu}{\partial x} = 0 \quad (1)$$

$$\frac{\partial hu}{\partial t} + \frac{\partial}{\partial x} \left(hu^2 + g \frac{h^2}{2} \right) + ghS_0 + \frac{\tau_T}{\rho_s} = 0 \quad (2)$$

where x =streamwise coordinate, t =time, g =gravity, h =layer depth, u =flow velocity, S_0 =bottom slope, ρ_s =material density, τ_T =total stress.

In the case of mixture of non-cohesive coarse fraction, the dissipation mechanism is influenced from the existence of two prevalent regimes (Johnson & Jackson 1987, Johnson et al. 1990): (a) a quasi-static regime, in which long-term contacts producing rubbing and sliding between particles occur; (b) a collisional regime, where the contacts are of short duration (Bagnold, 1954). For this reason, the total stress is written as the sum of two terms:

$$\tau_T = \tau_s + \tau_b = c_0 \rho_s \alpha u^2 + \rho_s g h \tan \varphi \quad (3)$$

where τ_s =collisional shear stress is expressed as the product of the square of the velocity, the Bagnold's coefficient α and the material bulk density $c_0 \rho_s$, being c_0 the volume fraction; τ_b =frictional shear stress is expressed by the Coulomb friction law, being φ a friction angle. It is worth of note that the τ_b term does not represent just the resistance on the bottom, since it is a depth integrated shear stress. In this framework, the evaluation of the friction angle is an important aspect that will be discussed later.

Equations (1) and (2) represent a system of conservation laws in the variables h and u . The investigation of the mathematical nature of the proposed model, reveals always the existence of two real and distinct eigenvalues:

$$\lambda_{1,2} = u \left(1 \pm \frac{1}{F} \right) \quad (4)$$

with $F = u / \sqrt{gh}$. Then, the total stress can be expressed as:

$$\tau_T = \tau_s + \tau_b = \tau_b \left(1 + \frac{\alpha c_0}{\tan \varphi} F^2 \right) \quad (5)$$

3 DAM BREAK TESTS

3.1 Experimental device and procedure

Dam break experiments were conducted in the Water Engineering Lab (LIA) of University of Cassino, using an apparatus consisting of a reservoir and an horizontal rectangular channel separated by a vertical fast opening sluice gate (Figure 1a).

The apparatus is made of smooth Perspex plates. The channel, after the gate, is 3 m long and both the reservoir and the channel are 0.40 m large. The gate is managed through a pneumatic system driven by a lever control, which allows high movement speeds. Transparent lateral walls allow for video analysis of the emptying reservoir and propagation of the flow in the channel. Two cameras were positioned in order to record from a sidewall and the top of the channel, respectively. The cameras have a resolution of 1360x1024 pixels and an acquisition frame rate of 30 fps. They are connected to a PC, from which they are managed. For each frame, the flow depth profile along the channel and the front position were evaluated through an image analysis technique.

a)

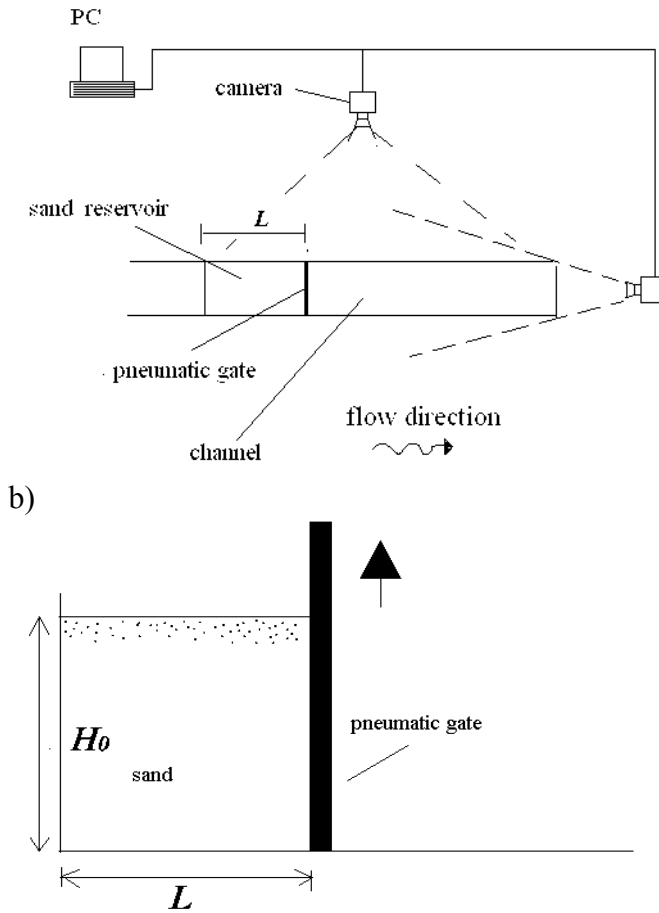


Figure 1. Sketch of the experimental device used (a), with the detail of the sand reservoir (b).

The granular material is sand of mean diameter 0.165 mm and density $\rho_s=2680 \text{ kg/m}^3$. The repose angle, obtained through laboratory tests, is 36° . For this kind of sand the cohesion can be considered negligible, anyway before the experiments grain particles were kept dry, in order to reduce such effect. Then, particles were poured into the reservoir with an initial estimated volume fraction $c_0=0.53$.

For all tests the reservoir length, L , was fixed equal to 0.5 m, while the initial column height, H_0 , was varied from 0.30 to 0.60 m (Figure 1b), so that the height-to-base aspect ratio $r=H_0/L$ is in the range 0.6-1.2 (Table 1). Test C was repeated three times to verify the reproducibility of the experiments. The comparison of the results of the three different collapses confirms that the tests are fairly reproducible.

From the analysis of video images recorded from the top of the channel the front position is detected. In order to facilitate such analysis the channel bottom was covered with graph paper. For all tests, top images (Figure 2) reveal also no significant wall effects on the depth, which is rather constant in the cross section. This observation confirms that the flows are fairly two-dimensional.



Figure 2. Image recorded from the top of the channel.

3.2 Numerical solution

From a mathematical standing point, the dam break problem consists in an instantaneous release at $t=0$ s of a semi-infinite expanse of static fluid of uniform depth H_0 into an initially dry region.

The numerical integration of the presented model is performed by a finite volume scheme described in Leopardi (2001), which uses a parabolic interpolation at the interfaces among adjacent cells and a predictor-corrector explicit time stepping. The method has a second-order accuracy both in space and time. This high accuracy of the method can produce spurious oscillations. In order to damp such oscillations an artificial diffusion term is added after each step, according to the implementation of Jameson et al. (1981).

For reproducing the experimental tests, in the numerical implementation closed wall and free flow are imposed as upstream and downstream boundary conditions, respectively. However, in the considered cases, as discussed in next paragraph, the results are not influenced by the assigned boundary conditions.

4 RESULTS

4.1 Experimental observations

For all performed tests, the column of sand collapses with a gradual transition from relatively slow fracture planes, along which material slide down. A surface wave propagates backward in the reservoir and the backward front stops before reaching the reservoir wall, leaving a portion of mass that does not move. This observation confirms that an infinite dam-break scheme can be assumed for the numerical simulations of the tests. As example, in Figure 3 the free surface profile at three different times for test C are reported. This behavior confirms what previously observed by

Balmforth & Kerswell (2005) for aspect ratios $r < 1.3$.

All realized flows form a final deposit whose longitudinal extent is lower than the channel length. While the final front position is clearly defined, the final runoff is more ambiguous. In fact, it is observed that after the collapse, when the slump comes to rest at the upward front, the backward wave still propagates in the channel (Figure 3). Material continues to adjust by avalanching of superficial layers, which decrease the upper surface slope until equilibrium is reached. The final upward front positions x_{sf} , and its stopping time (runoff), t_f , along with the total duration, t_t , of the phenomenon are reported in Table 1 for all tests. The front position is evaluated starting from the gate position, assumed at $x=0$ m. From the final longitudinal profile, reported in Figure 3, it is possible to observe a lower slope respect to the value of the repose angle (36°). This observation shows that the final configuration is not the equilibrium bank profile, but it depends on the dynamic of the phenomenon.

A more detailed analysis of the experimental data, also using scaling results, is reported in Di Cristo et al. (2010). In particular, assuming the initial column depth H_0 and $(H_0/g)^{1/2}$ as length and time scale respectively, the profiles describing the front development in time collapse, as shown in Figure 7.

Table 1. Final fronts positions x_{sf} , and stopping time, t_f , total duration, t_t , of the phenomenon for all tests.

Test	H_0 (m)	r	x_{sf} (m)	t_f (s)	t_t (s)
A	0.30	0.6	0.3825	0.73	4.19
B	0.40	0.8	0.5175	0.87	4.29
C	0.50	1	0.6025	1.00	4.43
D	0.60	1.2	0.6975	1.13	4.58

4.2 Comparison between experimental and numerical results

For the numerical reproduction the frictional stress is computed using $\varphi = 24^\circ$, equal to $2/3$ of the repose angle. The use of a value lower than 36° , suggests that the repose angle is not representative of the considered phenomenon. The Bagnold coefficient is $\alpha = 2.0$, fixed for all tests through a sensitivity analysis.

In Figure 3 the comparison between experimental and numerical free surface profiles at three times for test C is presented as example, but similar results are obtained also for the other tests. It can be observed that the simulated front position is faster than in the experiments in the very early stage of the phenomenon ($t = 0.36$ s). However the difference becomes negligible when the front

is going to stop ($t = 1.00$ s). At that stage also the shape of the simulated and measured profiles appears in reasonable agreement. The simulated backward front celerity appears higher than in the experiments.

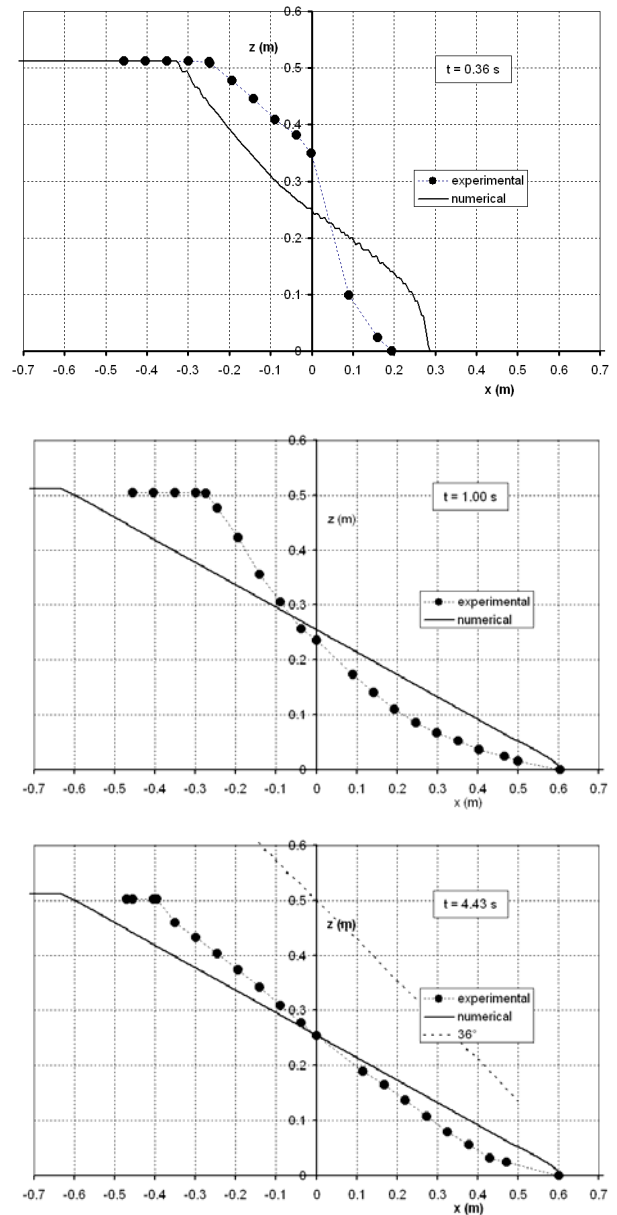


Figure 3. Free surface profiles at time $t=0.36$ s, $t=1.00$ s and $t=4.43$ s (final configuration) for test C ($H_0=0.50$ m). Gate position ($x=0$ m).

In the numerical simulation when the front stops the whole phenomenon ends. Such behaviour is different from the experimental evidence, that shows, after the stop of the front, a secondary adjustment process of the slope surface by avalanching of superficial layers, as described in paragraph 4.1. This difference is not surprising since the model is depth integrated. In fact the superficial movements of the sand could be taken into account only considering different velocities along the vertical direction. However, the final configuration ($t = 4.43$ s) produced by the numerical model is very close to the experimental one.

In other terms, even if the dynamic of the secondary slope adjustment process cannot be completely reproduced by the model, its final evolution is correctly forgone.

Above observations are confirmed by the Figure 4, that reports the comparison between the experimental front development in time and its numerical reproduction. It is confirmed that the numerical front position moves initially faster than the experimental one, but the stopping process of is reproduced in the right way.

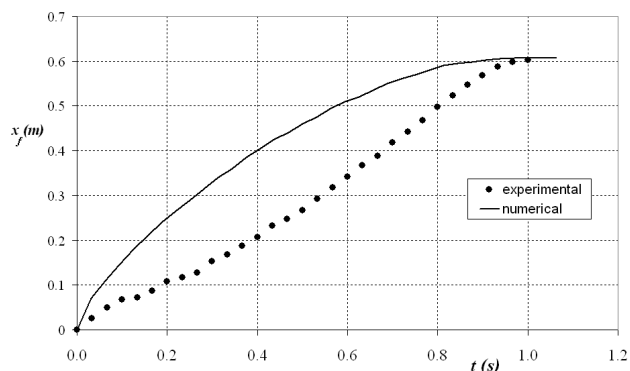


Figure 4. Front position versus time for test C ($H_0=0.50$ m) - Comparison between experimental and numerical data.

As said before, the described behavior is shared by all tests. It is confirmed by the results shown in Figures 5, 6 and 7. Figure 5 and 6 report for all tests the comparison between the experimental and numerical front stopping time and final position, respectively.

It can be observed from Figure 5 that the front stopping time is reproduced accurately in all tests, without performing any calibration of model parameters.

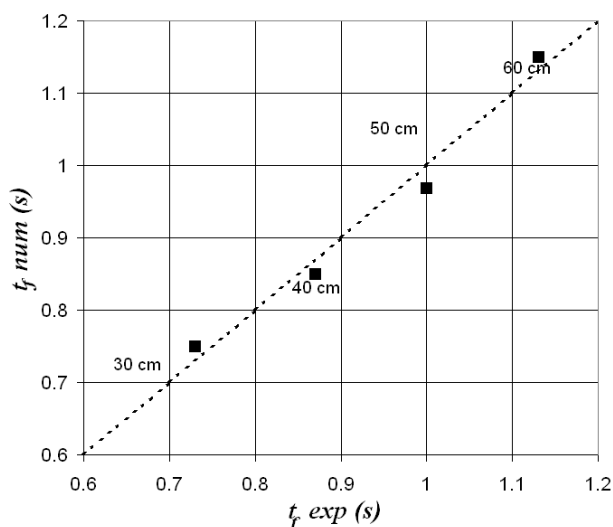


Figure 5. Stopping time of the front - Comparison between experimental and numerical data.

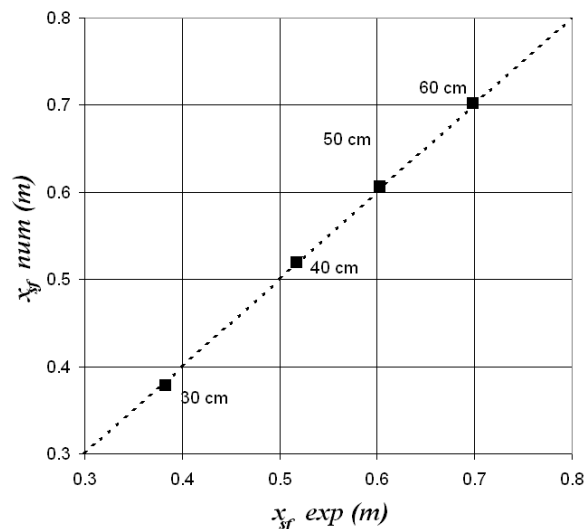


Figure 6. Final position of the front - Comparison between experimental and numerical data.

Also the final front position reproduction appears very good for all tests (Figure 6) and this result confirms the capability of the proposed model in reproducing the front advancing process.

Figure 7 reports the profiles describing the front development in time for all tests in the non-dimensional coordinates X and T defined as:

$$X = \frac{x_f}{H_0} \quad T = t \cdot \sqrt{\frac{g}{H_0}} \quad (6)$$

The collapse of the nondimensional profile for all performed tests demonstrates that an approximate Froude similarity exists among front position versus time for the height-to-base aspect ratio range investigated. The behavior observed for test C in Figure 4 is confirmed for the others: for all tests the numerical fronts move initially faster than the numerical ones in the very early stage of the phenomenon, but the stopping process is correctly reproduced.

5 CONCLUSIONS

In the present paper dry granular dam break flow is investigated through experimental laboratory tests. The experimental data are compared against the numerical simulated results of a depth-integrated model.

Experiments were conducted using an ad hoc experimental apparatus and digital images processing. In all tests the longitudinal extent of the final deposit is lower than the channel length, while the backward front stops before reaching the reservoir wall. It is also observed that after the collapse, when the slump comes to rest at the upward front, the backward wave still propagates in the channel. Material continues to adjust by avalanching of superficial layers, with a decreasing of

the upper surface slope until equilibrium is reached.

The presented numerical model, previously developed by some of the authors for two-phase flows, is here originally applied to granular flows. Such model accounts for sediment particles collisional shear stress through a kinetic scheme and frictional stress through a Coulomb-like behaviour.

Comparisons between experimental and numerical results show a good capability of the model of reproducing the front final position and stopping time. This is very important since in ap-

plication to real world problems it represents the most important feature.

Moreover the model can compute in an accurate way also the final configuration of the deposit. It cannot completely reproduce the dynamic of slope adjustment after that the upward front is at rest. This is due to the considered depth-integrated scheme, in which a constant velocity is assumed on a vertical column of sand. Further research will investigate on how to overcome this limitation.

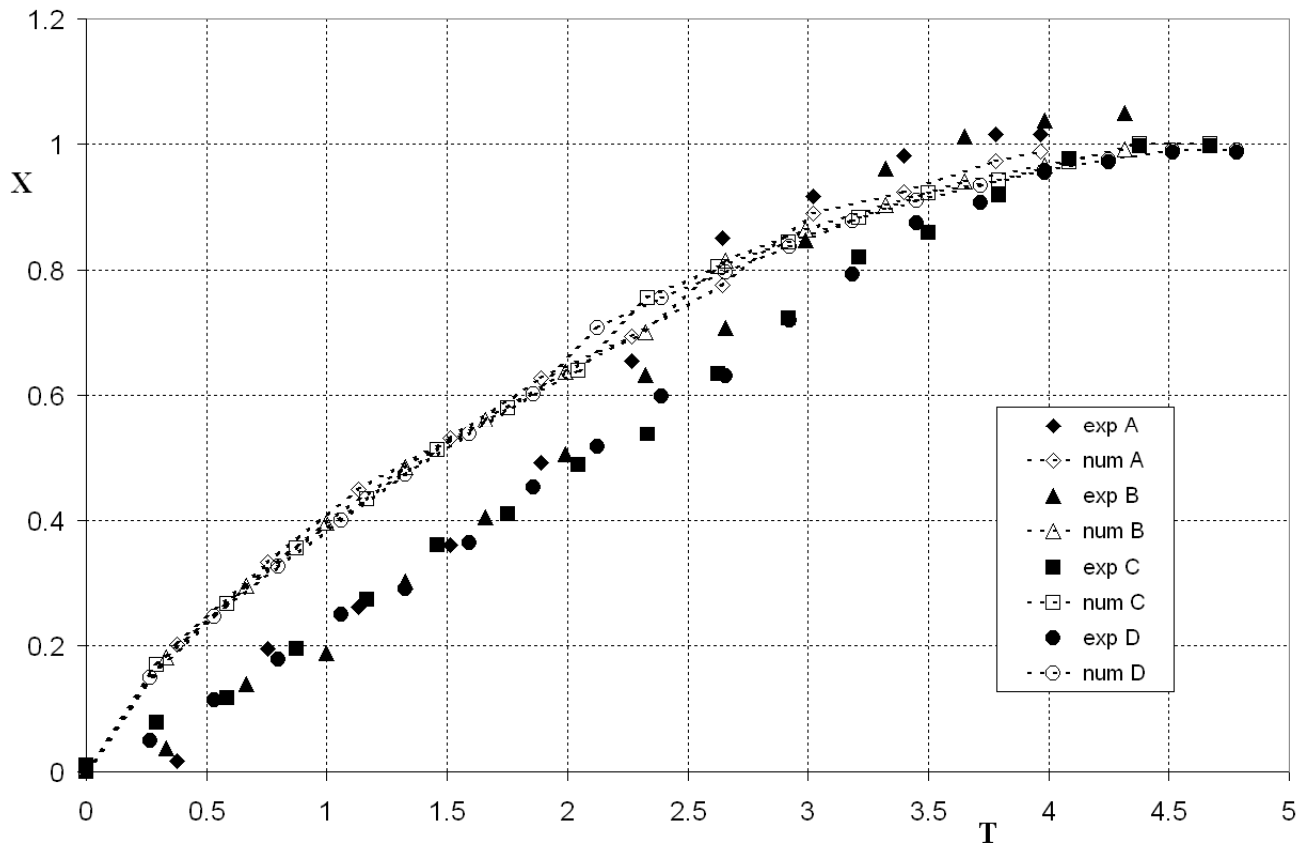


Figure 7. Front position versus time for all tests (non-dimensional coordinates).

REFERENCES

- Bagnold, R.A. 1954. Experiments on a gravity-free dispersion of large solid spheres in a Newtonian fluid under shear, *Proc. Roy. Soc.*, 225, 49-63.
- Balmforth, N.J., Kerswell, R.R. 2005. Granular collapse in two dimension. *J. Fluid Mech.*, 538,399-428; DOI: 10.1017/S0022112005005537
- Capart, H., Young, D. L. 1998 Formation of a jump by the dam-break wave over a granular bed. *J. Fluid Mech.* 372, 165-187.
- Chanson, H., Jarny S., Coussot, P. 2006. Dam break of thixotropic fluid. *J. of Hydr. Eng, ASCE*, 132(3), 280-293; DOI:10.1061/(ASCE)0733-9429
- Di Cristo, C., de Marinis, G., Vacca, A. 2010. Analytical solution of dam break wave in dry granular flows. *Proc. of the 1st European IAHR Congress, Edinburgh (UK).*
- Fracarollo, L. and Capart, H. 2002 Riemann wave description of erosional dam-break flows. *Journal of Fluid Mechanics*, vol. 461, pp. 183 – 228.
- Frenette, R., Zimmermann, T., Eyheramendy, D. 2002. Unified modeling of fluid or granular flows on dam-break case. *J. of Hydr. Eng, ASCE*, 128(3), 299-305;
- Graf, W.H., with M. Altinakar 1998. *Fluvial Hydraulics: Flow and Transport Processes in Channels of Simple Geometry.* John Wiley & Sons.
- Greco, M., Iervolino, M., Vacca, A., Leopardi, A. 2008. A two-phase model for sediment transport and bed evolution in unsteady river flow. *Proc. of River Flow 2008*, Altinakar, M. et al. (eds.), Çeşme, Turkey.
- Jameson, A., Schmidt, W. e Turkel, E. 1981. Numerical Solutions of the Euler Equations by Finite Volume Methods Using Runge-Kutta Time Stepping Schemes. – *AIAA 14th Fluid and Plasma Dynamics Conference*, Palo Alto, California, AIAA-81-1259.

- Johnson, P.C., Jackson, R. 1987. Frictional-collisional constitutive relations for granular materials, with application to plane shearing, *J. Fluid Mech*, 176, 67-93.
- Johnson, P.C., Nott, P., Jackson, R. 1990. Frictional-collisional equations of motion for particulate flows and their application to chutes, *J. Fluid Mech*, 210, 501-535
- Kerswell, R.R. 2005. Dam break with coulomb friction: a model for granular slumping? *Phys. Fluids*, 17; DOI:10.1063/1.1870592
- Lajeunesse, E., Mangeney-Castelnau, A., Vilotte, J.P. 2004. Spreading of a granular mass on a horizontal plane. *Phys. Fluids*, 16, 2371
- Leopardi, A. 2001 *Modelli Bidimensionali di Corpi Idrici Naturali*. University of Naples "Federico II", PhD Thesis.
- Lube, G., Huppert, H.E., Sparks, R.S.J., Hallworth, M.A. 2004. Axisymmetric collapses of granular columns. *J. FluidMech.*,508,175-199;DOI: 10.1017/S0022112004009036
- Lube, G., Huppert, H.E., Sparks, R.S.J., Freundt, A. 2005. Collapses of two dimensional granular columns. *Phys. Rev. E*,72,DOI: 10.1103/PhysRevE.72.041301
- Pouliquen, O. 1999. Scaling laws in granular flows down rough incline planes. *Phys. Fluids*, 11(3), 542-548; DOI: S1070-6631(99)00603-0
- Roche O., Montserrat, S., Nino, Y., Tamburrino, A. 2008. Experimental observations of water like behavior of fluidized, dam break granular flows and their relevance for the propagation of ash-rich pyroclastic flows. *J. of Geophys. Res.*, 113, 1-15; DOI:10.1029/2008JB005664
- Savage, S.B.,Hutter, K. 1989. The motion of a finite mass of granular material down a rough incline. *J. Fluid Mech.*, 199,177-215
- Spinewine, B., Zech, Y. 2007 Small-scale laboratory dam-break waves on movable beds, *Journal of Hydraulic Research*, 45 Extra Issue, 73-86.